Title

Study of the interactions between proximal femur 3d bone shape, cartilage health, and biomechanics in patients with hip Osteoarthritis

Journal

Journal of Orthopaedic Research®, 36(1)

ISSN

0736-0266

Authors

Pedoia, Valentina
Samaan, Michael A
Inamdar, Gaurav
et al.

Publication Date

2018

DOI

10.1002/jor.23649

Peer reviewed

HHS Public Access

Author manuscript

J Orthop Res. Author manuscript; available in PMC 2019 January 01.

Published in final edited form as:

J Orthop Res. 2018 January ; 36(1): 330–341. doi:10.1002/jor.23649.

Study of the Interactions Between Proximal Femur 3D Bone Shape, Cartilage Health and Biomechanics in Patients with Hip Osteoarthritis

Valentina Pedoia, PhD[1,*], **Michael A. Samaan, PhD**[1], **Gaurav Inamdar**[1], **Matthew C. Gallo, B.A**[1], **Richard B. Souza, PT, PhD**[1,2], and **Sharmila Majumdar, PhD**[1]

[1]Department of Radiology and Biomedical Imaging, University of California San Francisco, CA

[2]Department of Physical Therapy and Rehabilitation Science, University of California San Francisco, CA

Abstract

In this study quantitative MRI and gait analysis were used to investigate the relationships between proximal femur 3D bone shape, cartilage morphology, cartilage biochemical composition, and joint biomechanics in subject with hip Osteoarthritis (OA). Eighty subjects underwent unilateral hip MR-imaging: T1ρ and T2 relaxation times were extracted through voxel based relaxometry and bone shape was assessed with 3D MRI-based statistical shape modeling. In addition, 3D gait analysis was performed in seventy-six of the studied subjects. Associations between shape, cartilage lesion presence, severity and cartilage T1ρ and T2 were analyzed with linear regression and statistical parametric mapping. An ad-hoc analysis was performed to investigate biomechanics and shape associations. Our results showed that subjects with a higher neck shaft angle in the coronal plane (higher mode 1, coxa valga), thicker femoral neck and a less spherical femoral head (higher mode 5, pistol grip) exhibited more severe acetabular and femoral cartilage abnormalities, showing different interactions with demographics factors. Subjects with coxa valga also demonstrated a prolongation of T1ρ and T2. Subjects with pistol grip deformity exhibited reduced hip internal rotation angles and subjects with coxa valga exhibited higher peak hip adduction moment and moment impulse. The results of this study establish a clear relationship between 3D proximal femur shape variations and markers of hip joint degeneration – morphological, compositional, well as insight on the possible interactions with demographics and biomechanics,

[*]Corresponding Author Contact Details: Valentina Pedoia, Phone: 1 (415) 549-6136, valentina.pedoia@ucsf.edu, Address: 1700 Fourth Street, Suite 201, QB3 Building San Francisco, CA, 94107.

Authors Contributions

- Conception and design: Valentina Pedoia and Sharmila Majumdar.
- Collection and processing of data: Valentina Pedoia, Gaurav Inamdar, Matthew C. Gallo
- Analysis and interpretation of the data: Valentina Pedoia, Sharmila Majumdar, Michael A. Samaan, Richard B. Souza
- Drafting of the article: Valentina Pedoia, Gaurav Inamdar
- Obtaining funding: Sharmila Majumdar and Richard B. Souza.
- Final approval of the article: All the authors.

Conflict of Interest:
The authors involved in this study have research grant funding, which is listed in the Acknowledgements.

suggesting that 3D MRI-based bone shape maybe a promising biomarker of early hip joint degeneration.

Graphical Abstract

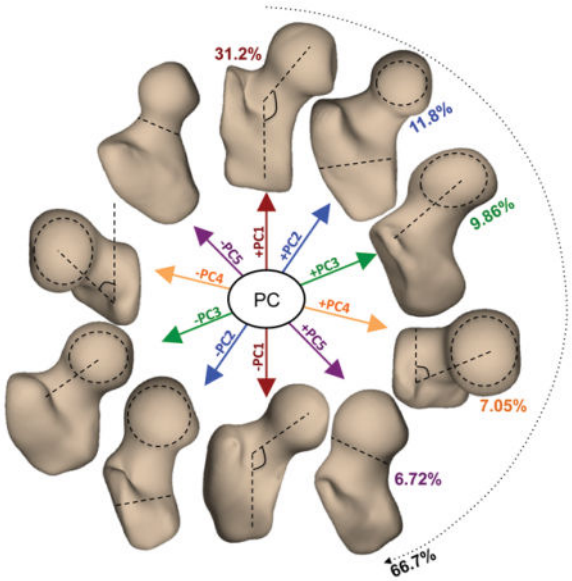

Keywords

MRI; Hip; Osteoarthritis (OA); Bone Shape; Statistical Shape Modeling (SSM); Cartilage; T1ρ/T2

INTRODUCTION

Hip osteoarthritis (OA) is a debilitating and degenerative joint disease and is highly prevalent in the United States due to an aging population as well as a growing number of obese individuals [1, 2]. Hip OA is characterized by a multifactorial pathogenesis and involves a huge social and economic impact, in addition to a significant negative effect on the individual's quality of life [3, 4].

It is well known that early stages of OA involves cartilage changes including proteoglycan loss, thinning and disruption of collagen, and changes in hydration; while late stages include dehydration and loss of cartilage accompanied by bone deformation [5]. T1ρ and T2 relaxation times provide a measure of proteoglycan content and collagen orientation [6–8], respectively, and prolongation in both these relaxation parameters were observed in hip OA subjects [9]. In addition, cartilage sub-regions characterized by elevated T1ρ and T2 values at baseline demonstrated longitudinal progression of morphological cartilage degeneration, indicating that T1ρ and T2 may be biomarkers for early OA [10]. The spatial variation of cartilage relaxation times in the hip joint, and the need for a regional analysis to extract a realistic imaging biomarker from relaxation parametric maps has also been recognized [11, 12]. In an attempt to address this challenge, voxel based relaxometry (VBR) [13] has been

recently proposed for the hip joint and was adopted to study the local association between T1ρ and T2 relaxation times and longitudinal changes in patient-reported outcomes [14].

In addition to early biochemical cartilage changes in hip OA, it has been suggested that changes also occur in the subchondral and trabecular bone. Articular cartilage and subchondral bone act in tandem with regards to the mechanical loading of the joint. The subchondral mineralized zone plays an important role in reducing the impact forces typically encountered during dynamic joint loading and adapts to the mechanical demands during normal and abnormal joint loading [15–17]. Both early-stage increased bone remodeling and bone loss, as well as, the late-stage reduced bone remodeling and subchondral densification are important components of the pathological process that leads to OA.

Previous work has used MRI and biomechanical analyses to assess the effects of hip joint abnormalities [18–20] and femoroacetabular impingement (FAI) [21–23] on hip joint mechanics during various activities of daily living (ADL). More specifically, FAI patients demonstrated increased hip joint loading during gait and these increased loading patterns within FAI patients were associated with increased severity of acetabular cartilage abnormalities. Also, the morphological abnormality present at the femoral-head neck junction (cam-type FAI) produces increased stress in the acetabular cartilage and labrum, which may lead to hip joint degeneration. These biomechanical studies demonstrate that altered hip joint morphology as well as the presence of cartilage degeneration alters hip joint mechanics during ADL yet a more comprehensive understanding of hip joint morphology and its association with hip joint mechanics and cartilage degeneration is needed.

There has been a growing interest in the analysis of bone shape as an early knee and hip OA imaging biomarker, with the majority of the applications being based on radiographic 2D analysis [24–27]. While 3D bone shape analysis using MRI has the potential to extract more detailed shape features, challenges such as segmenting the bone and other tissues becomes time intensive if done manually, or even semi-automatically [28–31]. Despite this constraint Three-dimensional Statistical Shape Modeling (SSM) has been increasingly employed in studies involving knee and hip OA [28–32].

Although shape features as possible early OA imaging biomarkers have been studied, there have been limited studies that aim to explore the relationships between proximal femur 3D bone shape and morphological and biochemical changes in articular cartilage in OA. Clearly, a better understanding of the role of bone shape in the cartilage degeneration process, which modulate the forces at work within the joint, is essential in order to gain insight into the mechanical causes of osteoarthritis of the hip.

In an attempt to fill this gap, the present study used quantitative imaging and gait analysis to: (i) evaluate the relationships between proximal femur bone shape and the presence of cartilage abnormalities detected with morphological MRI; (ii) to analyze the local patterns of $T_{1\rho}$ and T_2 relaxation time elevations in association with specific bone shape variations using voxel-based relaxometry and (iii) study the associations between bone shape features related to cartilage health and gait biomechanics, with the aim to improve the interpretation of the results in (i) and (ii).

We hypothesized that specific bone shape features are associated with the presence of femoral and acetabular cartilage abnormalities and prolongation in T1ρ and T2 relaxation times, indicating changes in cartilage biochemistry shown to be consistent with the onset of OA. We also hypothesized that these shape variations are associated with hip joint mechanics.

METHODS

This is an analytic study (Level of Evidence: III). All subjects provided written informed consent, and the study was carried out in accordance with the regulations of the Committee for Human Research at our institution.

Subjects

Subjects in the current study were part of a longitudinal study on hip OA. Participants were excluded if they were below the age of 18, had a history of previous hip trauma, inflammatory arthritis, hemochromatosis, sickle cell disease, or hemoglobinopathy, hip joint Kellgren and Lawrence (KL) score > 3, contraindications to MRI, radiographic evidence of femoroacetabular impingement or any spine or lower extremity conditions that would negatively affect their ability to perform the dynamic tasks during the data collection.

Weight bearing anterior-posterior radiographs of each participant were obtained and used by an experienced musculoskeletal radiologist to assign bilateral KL scores and to measure neck shaft angle and alpha angle The hip with the higher KL score was used as the study hip and underwent an MRI. If both hips had the same KL, the side imaged using MR was selected randomly.

Imaging Protocol

Hip MR images were obtained using a 3T scanner (GE MR750; GE Healthcare, Waukesha, WI) using an 8-channel receive-only cardiac coil (GE Healthcare, Waukesha, WI). Subjects were positioned supine and hip joint position was standardized: feet were slightly internally rotated and taped together to prevent movement during the scan [11]. The MRI protocol adopted for this study is descried in Table 1. Semi-quantitative clinical grading of acetabular and femoral cartilage abnormalities was performed using the Scoring Hip Osteoarthritis with MRI (SHOMRI) scoring system [33, 34].

Image Processing: 3D Shape Analysis

All image processing was performed using an in-house program developed in Matlab (The Mathworks, Natick, MA). The proximal femurs of all the subjects were segmented automatically on the T1ρ-weighted image with TSL = 0 using a single atlas-based method [13] refined by active contours. All the segmentations underwent a strict protocol of quality control and a single user (GI) manually adjusted the bone segmentation in case of failure of the automatic procedure. 3D-SSM was performed as previously described and evaluated [35, 36].

Image Processing: T1ρ and T2 Voxel-Based Relaxometry

T1ρ and T2 relaxation times were automatically analyzed with a previously proposed and evaluated technique [14]. Briefly, all the T1ρ-weighted and T2-weighted images were non-rigidly registered on a single reference identified through an iterative process aimed to minimize global image deformation. T1ρ and T2 maps were then obtained by fitting the morphed images obtained with different TSL and TE. The alignment of all subjects onto a single template allowed for voxel-based statistical analysis (Statistical Parametric Mapping).

Gait Analysis

Three-dimensional lower extremity joint kinematics and kinetics were obtained for 76 of the 80 subjects while walking at a self-selected speed. A 10-camera motion capture system (VICON, Oxford Metrics, Oxford, UK) was used to obtain 3D position data at a sampling rate of 250 Hz, while ground reaction forces were obtained simultaneously using two embedded force platforms (AMTI, Watertown, MA, USA) at a sampling rate of 1000 Hz. Fourteen-millimeter spherical reflective markers were used to determine segment lengths and joint centers and placed at L5/S1 and bilaterally at the iliac crests, anterior superior iliac spines, greater trochanters, medial and lateral femoral condyles, medial and lateral malleoli, first and fifth metatarsal heads. In addition, rigid marker clusters were placed bilaterally on the thighs, shanks and heel shoe counters to track segment position. A one second standing calibration trial was obtained for each subject.

Each subject was asked to perform three successful walking trials at a self-selected speed. A trial was considered successful if the subject's foot made a clean strike on a force plate and the subject's speed was maintained within 5% of their first successful trial. All raw marker position and ground reaction force data were processed using a 4^{th} order Butterworth filter at 6Hz and 50Hz, respectively. A seven segment kinematic model (i.e. pelvis, thighs, shanks and feet) was created from the standing calibration trial using Visual3D (C-Motion, Germantown, MD). Inverse dynamics was used to compute external net joint moments and were normalized by body mass (Nm/kg) [37]. Hip joint angles and moments were assessed during the stance phase of gait and the hip joint moment impulse (Nm*ms/kg) was computed as the integral of a particular portion of the hip joint moment curve with respect to time (ms). Active range of motion tests were performed at the same time as gait analysis in order to assess: hip flexion angle and hip internal rotation.

Statistical Analysis

Stepwise linear regression was used to study the associations between the first five bone shape modes and the SHOMRI cartilage scores in acetabular and femoral cartilage, joint biomechanics and active range of motion tests. The model was performed with and without demographics (age, gender and BMI) as possible predictors, with the aim of studying the additional information derived by the inclusion of shape features over the demographics and the exploration of potential interactions between shape and demographic factors. Ad-hoc analysis was performed with the aim of testing if the complex 3D MRI-based features could complement, or overcome the easier extractable 2D radiograph-based feature. Stepwise regression models including both 2D and 3D measurements were tested in association with presence of cartilage lesions.

Voxel-based Pearson partial correlation adjusted for age, gender and BMI was performed to study the local association between bone shape features and T1ρ and T2 relaxation time. A p-value of 0.05 was considered as significant threshold.

RESULTS

Eighty subjects (37 female, 43 male) were considered for this study (age 47.0 ± 13.4 years, BMI 23.8 ± 3.1 kg/m^2). Of these 80 subjects, 42 (52.5%) had a KL score greater than 1 indicating radiographic hip OA. Fifty-two (65%) subjects showed the presence of femoral or acetabular cartilage abnormalities as determined by the SHOMRI score. Table 2 reports the overall baseline MRI characteristics of this dataset evaluated by SHOMRI.

The first five shape modes (Figure 1) described 66.7% of the overall variation within the dataset and were considered for further analysis. Mode 1 alone described 31.2% of the total variability within the analyzed dataset. Higher values of mode 1 corresponded to a larger neck shaft angle in the coronal plane and have been shown in previous studies to relate a condition known as coxa valga [38]. On the contrary, lower values of mode 1 correspond to a condition known as coxa vara [38]. Mode 2 (11.8 %) was related to the ratio between the femoral head radius and the shaft thickness while variations of mode 3 (9.86%) changed the medial–lateral length of the femoral neck. Higher values of mode 4 (7.05%) were related to larger neck shaft angle in the axial plane. Higher values of mode 5 (6.72%) corresponded to a thicker femoral neck and less spherical femoral head and is related to a condition known as pistol grip deformity [38]. In addition, higher values in mode 5 were observed in men and in subjects with higher BMI. While visual examination of the 3D modeling may make it possible to determine the dominant feature that each mode represents, the subtle features, secondary characteristics that may affect the modes are not often visually discernable; 3D SSM is a methodology that makes it easy to describe 3D complex deformations that are not easily represented by simple geometric measurements.

Mode 1 and mode 5 were observed to be significant predictors of the presence and severity of cartilage abnormalities in the acetabular (P-value = 0.0016) and femoral cartilage (P-value = 0.0032, Table 3A), when demographics are not considered in the model. Subjects with coxa valga and pistol grip deformities exhibited higher average SHOMRI cartilage abnormality scores. When age, gender and BMI were considered as independent variables in the model (Table 3B), mode 1 (P-value = 0.01), remained a significant predictor of femoral cartilage abnormalities but mode 5 was not significant for femoral or acetabular abnormalities. In addition, we observed a significant (P-value = 0.02) interaction between age and shape mode 1 in the prediction of femoral cartilage abnormalities. The loss of significant in mode 5 is related to the association between this shape feature and both gender and BMI. Male subjects and subjects with higher BMI demonstrate higher values in mode 5 (thicker femoral neck).

When mode 1 and radiographic measures of neck shaft angle were simultaneously considered in the stepwise regression model (Table 3C), mode 1 shown to be a better predictor of acetabular cartilage lesion SHOMRI grades than the 2D neck shaft angle, which was not included in the model; however both the 2D geometrical features (P-value = 0.01)

and 3D SSM feature (P-value = 0.04) contributed to the prediction of femoral cartilage lesion SHOMRI grades (model P-value = 0.0037). Similarly the addition of mode 5 in addition to the radiographic measure of alpha angle, and the interaction between those 2 variables improved the prediction of acetabular cartilage lesion grades. While the 3D bone shape was not included in the femoral cartilage lesion model when alpha angle was considered.

Although both mode 1 and mode 5 were positively associated with SHOMRI scores, a different interaction with demographics was observed and a clear dichotomy was seen between values of the two modes. Mode 1 values were more distinguished at lower SHOMRI scores (Figure 2A–2C), while mode 5 values were more distinguished at higher SHOMRI scores (Figure 2B–2D).

When the first 5 modes were evaluated in association with T1ρ and T2 relaxation times, we observed significant positive associations between mode 1 and T1ρ in 29.05% of the acetabular voxels with an average R-value = 0.36 and in 34.46% of the femoral voxels with an average R-value = 0.38, (Table 4). Subjects with coxa valga deformity exhibited a prolongation in relaxation times. Upon observing the R-value and P-value statistical parametric maps (Figure 3A), there was a notable concentration of strongly correlated voxels in the more medial aspect of the hip cartilage and were mainly focused in the anterior superior and posterior superior regions of the hip joint. A similar pattern was observed for T2, however the clusters of significant voxels were smaller in both the acetabular (PSV =17.63%) and femoral cartilage (PSV=14.97%). A small cluster of significant negative voxels were also observed in the more lateral aspect in both T1ρ (acetabular PSV=6.22%, femoral PSV=3.68%) and T2 (acetabular PSV=6.76%, femoral PSV=15.07%) suggesting a relationship with the loading distribution and this specific bone variation. None of the other shape modes showed relevant associations with T1ρ or T2 relaxation times.

For a more comprehensive understanding of these results the associations between mode 1 and mode 5 with hip joint angles, moments and moment impulses during gait and hip internal rotation and hip flexion active range of motion tests were evaluated. Table 5A and 5B show the results of these analyses. Subjects with higher mode 5 (pistol grip deformity) exhibited a smaller hip internal rotation angle when evaluated in both gait analysis (Table 5A) and clinical testing (Table 5B), while both gender and mode 1 were significant predictors of the peak external hip adduction moment and moment impulse none of the evaluated shape showed a significant association with hip flexion angle.

DISCUSSION

In this study we demonstrated the ability of 3D Statistical Shape Modeling to quantify hip bone shape features from MRI. We observed that bone shapes were associated with morphological and biochemical degeneration of the articular cartilage and may be early signs of hip OA. We also observed associations between bone shapes with hip joint mechanics during gait.

Previous studies have used radiographs to establish a clear link between certain proximal femur bone shapes and OA [39, 40]. Our results confirmed these previous studies, showing further evidence of the critical role of the bone shape in the development of OA and of the ability of MRI and 3D shape modeling to quantify those features.

Specifically we observed that higher values in the bone shape feature mode 1, related to the condition of coxa valga, predicted the presence and severity of cartilage abnormalities and demonstrated interaction with gender in this association. In addition, subjects that exhibited this bony deformity showed a prolongation in T1ρ and T2 relaxation times and higher hip adduction moment and moment impulse. This coupled with the ability of mode 1 in distinguishing lower values of SHOMRI cartilage scores suggests that this shape feature might be a good indicator of early OA progression or a possible morphological risk factor of OA. The higher neck shaft angle of the coxa valga shape has been associated with reduced gluteus medius moments arms [41] and therefore may be related to altered frontal plane hip joint loads during weight bearing activities [42] These changes in gait mechanics and loading, along with the altered bony morphology of the proximal femur, may contribute to cartilage degeneration.

The femoral neck-shaft angle (NSA) is widely studied and discussed in OA research yet these results are contradictory and currently, there is no consensus on the relationship between hip joint shape variation and OA. A study conducted by Javaid et. al used radiographic images to measure certain geometric features and their relationship to OA [43] and did not observe a relationship between hip OA and the neck shaft angle. Another study measured geometric parameters on radiographs and observed that a higher NSA was related to incidence of OA [44]. While our results may suggest coxa valga as a possible early manifestation of OA or even a geometrical risk factor, a study conducted by Doherty et al. [21] performed on radiographs exhibited the opposite results as the current study. This study demonstrated that the coxa vara shape is a possible predictor of hip OA while the coxa valga shape occurs as a result of OA [24]. However, a study conducted by Benlidayi et al. exhibited differing results, as it was observed that patients with higher NSA exhibited sever knee OA and that people with a NSA of above 134.4° have eightfold increased risk of developing knee OA [45]. Despite the contradictory results of previous studies, the results of the current study suggest that a higher NSA is related to hip joint cartilage degeneration and may be an indicator of the early signs of hip OA yet should be further evaluated using a longitudinal study, in order to better understand the relationship between proximal hip joint shape and cartilage degeneration.

In addition to the cross-sectional association with the presence of cartilage abnormalities, mode 1 was observed to be correlated with T1ρ and T2 values in the anterior superior and posterior superior regions of the hip joint cartilage and suggests that subjects with the coxa valga deformity exhibit a prolongation in relaxation times. T1ρ and T2 values in these specific cartilage regions were previously observed to be significant predictors of the longitudinal progression of cartilage lesions [10], suggesting, as a possible future direction, the combined use of shape analysis and compositional MRI to improve the predictive ability of longitudinal cartilage degeneration.

In our study we also observed a prevalence of higher values of mode 5 in subjects with more severe cartilage abnormalities. Higher values in mode 5 has been shown to be correlated to a thicker femoral neck and is related to a condition known as pistol grip deformity [24]. It is also worth noting that while subjects with higher mode 5 showed a 3D shape deformation, from MRI analysis, similar to FAI, the subjects were excluded in this study and do not meet the criteria as FAI based on radiographic inspection (alpha angle); this may partially explain the lack of differences observed. However, our results indicate that mode 5 is not a proper indicator of the early signs of cartilage degeneration (i.e. no relationship with T1ρ or T2 relaxation times) but mode 5 can distinguish severity in cartilage abnormalities in the later OA stages.

The results of the current study demonstrated that mode 5 was related to gender and BMI and help to confirm the results of the Doherty et. al study, in which the pistol grip shape was found to be more common among men [24]. Also, a previous study conducted by Agricola et.al used SSM confirmed that a thicker femoral neck is related to incidence of OA [46]. However, further studies are still required to observe the interactions between this shape variation and gender/BMI in the prediction of cartilage lesions.

We also observed a significant association between mode 1 and gender with the peak external hip adduction moment and moment impulse as well as an association of mode 5 with the peak hip internal rotation angle during gait. Previous work has demonstrated that an increased peak external hip adduction moment during gait was a protective mechanism of medial knee joint OA progression [47]. The subjects in the current study demonstrated similar hip joint loading patterns as those observed in the Chang et al. study [47] and may be reducing the medial knee joint load. The coxa vara deformity may be causing the subjects in the current study to apply increased hip joint contact forces, due to the increased hip abductor moment arm and, thereby leading to the observed cartilage degeneration in the medial aspects of the hip joint. Also, the increased external hip adduction moment impulse may be detrimental to the hip joint cartilage, as the subjects with coxa valga continuously apply larger hip joint loads over multiple strides of the gait cycle. Females possess larger quadriceps (Q-angles) compared to males and this difference in frontal plane alignment may affect the moment arms of the hip joint abductors and help to explain the association between mode 1 and gender with hip frontal plane loading.

Previous studies that aimed to understand the contribution of shape to OA mainly used radiographs to quantify bone shape and to define OA. Using plain radiographs to study the association between bone shape and OA has two main disadvantages: (i) assessing shape features on a 2D projection may be affected by the joint positioning during the acquisition and the simplification of a 3D object on a 2D plane cannot capture the real shape complexity; (ii) radiographic changes of OA, such as joint space narrowing and presence of osteophytes, are late manifestation of the disease; and are not optimal biomarkers to study early degeneration and pathogenesis.

The coupling between quantitative MRI (i.e. cartilage morphology and composition) and 3D statistical shape modeling, as proposed in the current study, has the potential to complement

the previous results obtained with 2D approaches and to shed light on the role of bone shape in understanding the pathogenesis of hip OA.

Despite the promising results, there are several limitations in the current study that need to be considered. The cross-sectional design of this study does not allow for establishing the temporal order of events, but allows for the observation of the associations between different aspects involved in hip OA such as bone shape, cartilage morphology and cartilage composition. The analysis of the bone shape is performed on an image with low resolution acquired with a large slice thickness (4mm). The acquisition and reconstruction of these images on smaller, isotropic voxels could allow for the analysis of more localized shape features ranked in later modes that are not reliably detectable at the current resolution and were not considered as part of this study. Joint loading is not only affected by the shape of the proximal femur, but also the shape of the acetabulum; images acquired with higher resolution could allow for a reliable assessment of both the bones shapes. While the usage of voxel based relaxometry revealed local patterns of T1ρ and T2 prolongation, the technique was not adopted for the analysis of local heterogeneity. Standard deviation and texture analyses, in addition to a more focused analysis of regional differences, would be of interest to extract subtler relaxometry changes. Future studies with longitudinal follow-up larger sample sizes are required to gain a better understanding of the biomechanical changes related with shape features and how these biomechanical patterns can affect cartilage health and whether or not bone shape features can be used to predict hip OA progression. Nevertheless, the relationships presented in this study provide new information regarding associations between 3D bone shape and cartilage degeneration and suggest the usage of 3D MRI-based bone shape as a promising early imaging biomarker for the study of hip OA.

Acknowledgments

We would like to thank: Sonia Lee, MD and Thomas M. Link, MD for their help with radiograph and MRI grading; Cory Wyatt and Deepak Kumar for their help in data collection. This study was supported by NIH NIAMS P50 AR060752 and F32 AR069458. The content of this study is solely the responsibility of the authors and does not necessarily represent the official views of the National Institutes of Health.

References

1. Berenbaum F, Eymard F, Houard X. Osteoarthritis, inflammation and obesity. Curr Opin Rheumatol. 2013; 25:114–118. [PubMed: 23090672]
2. Lee J, Song J, Hootman JM, Semanik PA, Chang RW, Sharma L, et al. Obesity and other modifiable factors for physical inactivity measured by accelerometer in adults with knee osteoarthritis. Arthritis Care Res (Hoboken). 2013; 65:53–61. [PubMed: 22674911]
3. Lawrence RC, Felson DT, Helmick CG, Arnold LM, Choi H, Deyo RA, et al. Estimates of the prevalence of arthritis and other rheumatic conditions in the United States. Part II. Arthritis Rheum. 2008; 58:26–35. [PubMed: 18163497]
4. Salaffi F, Carotti M, Stancati A, Grassi W. Health-related quality of life in older adults with symptomatic hip and knee osteoarthritis: a comparison with matched healthy controls. Aging Clin Exp Res. 2005; 17:255–263. [PubMed: 16285189]
5. Li X, Majumdar S. Quantitative MRI of articular cartilage and its clinical applications. J Magn Reson Imaging. 2013; 38:991–1008. [PubMed: 24115571]
6. Nieminen MT, Rieppo J, Toyras J, Hakumaki JM, Silvennoinen J, Hyttinen MM, et al. T2 relaxation reveals spatial collagen architecture in articular cartilage: a comparative quantitative MRI and polarized light microscopic study. Magn Reson Med. 2001; 46:487–493. [PubMed: 11550240]

7. Akella SV, Regatte RR, Wheaton AJ, Borthakur A, Reddy R. Reduction of residual dipolar interaction in cartilage by spin-lock technique. Magn Reson Med. 2004; 52:1103–1109. [PubMed: 15508163]
8. Li X, Cheng J, Lin K, Saadat E, Bolbos RI, Jobke B, et al. Quantitative MRI using T1rho and T2 in human osteoarthritic cartilage specimens: correlation with biochemical measurements and histology. Magn Reson Imaging. 2011; 29:324–334. [PubMed: 21130590]
9. Wyatt C, Kumar D, Subburaj K, Lee S, Nardo L, Narayanan D, et al. Cartilage T1rho and T2 Relaxation Times in Patients With Mild-to-Moderate Radiographic Hip Osteoarthritis. Arthritis Rheumatol. 2015; 67:1548–1556. [PubMed: 25779656]
10. Gallo MC, Wyatt C, Pedoia V, Kumar D, Lee S, Nardo L, et al. T1rho and T2 relaxation times are associated with progression of hip osteoarthritis. Osteoarthritis Cartilage. 2016; 24:1399–1407. [PubMed: 26973330]
11. Anwander H, Rakhra KS, Melkus G, Beaule PE. T1rho Hip Cartilage Mapping in Assessing Patients With Cam Morphology: How Can We Optimize the Regions of Interest? Clin Orthop Relat Res. 2016
12. Subburaj K, Valentinitsch A, Dillon AB, Joseph GB, Li XJ, Link TM, et al. Regional variations in MR relaxation of hip joint cartilage in subjects with and without femoralacetabular impingement. Magnetic Resonance Imaging. 2013; 31:1129–1136. [PubMed: 23684960]
13. Pedoia V, Li X, Su F, Calixto N, Majumdar S. Fully automatic analysis of the knee articular cartilage T1rho relaxation time using voxel-based relaxometry. J Magn Reson Imaging. 2016; 43:970–980. [PubMed: 26443990]
14. Pedoia V, Gallo MC, Souza RB, Majumdar S. Longitudinal study using voxel-based relaxometry: Association between cartilage T1rho and T2 and patient reported outcome changes in hip osteoarthritis. J Magn Reson Imaging. 2016
15. Muller-Gerbl M, Griebl R, Putz R, Golman A, Kuhr M, Taeger K. Assessment of subchondral bone density distribution patterns in patients subject to corection osteotomy. Trans Orth Society. 1994; 19:574.
16. Muller-Gerbl M, Putz R, Hodapp N, Schulte E, Wimmer B. Computer tomography osteo-absorptiometry for assessing the density distribution of subchondral bone as a measure of long term mechanical adaptation in individual joints. Skeletal Radiology. 1989; 18:507–512. [PubMed: 2588028]
17. Pauwels, F. Biomechanics of the locomotor apparatus. Berlin: Springer; 1980.
18. Kumar D, Wyatt C, Chiba K, Lee S, Nardo L, Link TM, et al. Anatomic correlates of reduced hip extension during walking in individuals with mild-moderate radiographic hip osteoarthritis. J Orthop Res. 2015; 33:527–534. [PubMed: 25678302]
19. Samaan MA, Teng HL, Kumar D, Lee S, Link TM, Majumdar S, et al. Acetabular cartilage defects cause altered hip and knee joint coordination variability during gait. Clin Biomech (Bristol, Avon). 2015; 30:1202–1209.
20. Samaan MA, Schwaiger BJ, Gallo MC, Link TM, Zhang AL, Majumdar S, et al. Abnormal Joint Moment Distributions and Functional Performance During Sit-to-Stand in Femoroacetabular Impingement Patients. PM R. 2016
21. Samaan MA, Schwaiger BJ, Gallo MC, Sada K, Link TM, Zhang AL, et al. Joint Loading in the Sagittal Plane During Gait Is Associated With Hip Joint Abnormalities in Patients With Femoroacetabular Impingement. Am J Sports Med. 2016 363546516677727.
22. Kumar D, Dillon A, Nardo L, Link TM, Majumdar S, Souza RB. Differences in the association of hip cartilage lesions and cam-type femoroacetabular impingement with movement patterns: a preliminary study. PM R. 2014; 6:681–689. [PubMed: 24534097]
23. Hunt MA, Guenther JR, Gilbart MK. Kinematic and kinetic differences during walking in patients with and without symptomatic femoroacetabular impingement. Clin Biomech (Bristol, Avon). 2013; 28:519–523.
24. Doherty M, Courtney P, Doherty S, Jenkins W, Maciewicz RA, Muir K, et al. Nonspherical femoral head shape (pistol grip deformity), neck shaft angle, and risk of hip osteoarthritis: a case-control study. Arthritis Rheum. 2008; 58:3172–3182. [PubMed: 18821698]

25. Waarsing JH, Rozendaal RM, Verhaar JA, Bierma-Zeinstra SM, Weinans H. A statistical model of shape and density of the proximal femur in relation to radiological and clinical OA of the hip. Osteoarthritis Cartilage. 2010; 18:787–794. [PubMed: 20171297]
26. Nelson AE, Liu F, Lynch JA, Renner JB, Schwartz TA, Lane NE, et al. Association of incident symptomatic hip osteoarthritis with differences in hip shape by active shape modeling: the Johnston County Osteoarthritis Project. Arthritis Care Res (Hoboken). 2014; 66:74–81. [PubMed: 23926053]
27. Wise BL, Kritikos L, Lynch JA, Liu F, Parimi N, Tileston KL, et al. Proximal femur shape differs between subjects with lateral and medial knee osteoarthritis and controls: the Osteoarthritis Initiative. Osteoarthritis Cartilage. 2014; 22:2067–2073. [PubMed: 25194496]
28. Bredbenner TL, Eliason TD, Potter RS, Mason RL, Havill LM, Nicolella DP. Statistical shape modeling describes variation in tibia and femur surface geometry between Control and Incidence groups from the osteoarthritis initiative database. J Biomech. 2010; 43:1780–1786. [PubMed: 20227696]
29. Neogi T, Bowes MA, Niu J, De Souza KM, Vincent GR, Goggins J, et al. Magnetic resonance imaging-based three-dimensional bone shape of the knee predicts onset of knee osteoarthritis: data from the osteoarthritis initiative. Arthritis Rheum. 2013; 65:2048–2058. [PubMed: 23650083]
30. Hunter D, Nevitt M, Lynch J, Kraus VB, Katz JN, Collins JE, et al. Longitudinal validation of periarticular bone area and 3D shape as biomarkers for knee OA progression? Data from the FNIH OA Biomarkers Consortium. Ann Rheum Dis. 2015
31. Bowes MA, Vincent GR, Wolstenholme CB, Conaghan PG. A novel method for bone area measurement provides new insights into osteoarthritis and its progression. Ann Rheum Dis. 2015; 74:519–525. [PubMed: 24306109]
32. Chan EF, Farnsworth CL, Koziol JA, Hosalkar HS, Sah RL. Statistical shape modeling of proximal femoral shape deformities in Legg-Calve-Perthes disease and slipped capital femoral epiphysis. Osteoarthritis Cartilage. 2013; 21:443–449. [PubMed: 23274103]
33. Lee S, Nardo L, Kumar D, Wyatt CR, Souza RB, Lynch J, et al. Scoring hip osteoarthritis with MRI (SHOMRI): A whole joint osteoarthritis evaluation system. J Magn Reson Imaging. 2015; 41:1549–1557. [PubMed: 25139720]
34. Schwaiger BJ, Gersing AS, Lee S, Nardo L, Samaan MA, Souza RB, et al. Longitudinal assessment of MRI in hip osteoarthritis using SHOMRI and correlation with clinical progression. Semin Arthritis Rheum. 2016; 45:648–655. [PubMed: 27162009]
35. Pedoia V, Lansdown DA, Zaid M, McCulloch CE, Souza R, Ma CB, et al. Three-dimensional MRI-based statistical shape model and application to a cohort of knees with acute ACL injury. Osteoarthritis Cartilage. 2015; 23:1695–1703. [PubMed: 26050865]
36. Pedoia V, Su F, Amano K, Li Q, McCulloch CE, Souza RB, et al. Analysis of the articular cartilage T1rho and T2 relaxation times changes after ACL reconstruction in injured and contralateral knees and relationships with bone shape. J Orthop Res. 2016
37. Winter DA. Biomechanics of human movement with applications to the study of human locomotion. Crit Rev Biomed Eng. 1984; 9:287–314. [PubMed: 6368126]
38. Baker-LePain JC, Lane NE. Relationship between joint shape and the development of osteoarthritis. Curr Opin Rheumatol. 2010; 22:538–543. [PubMed: 20644480]
39. Lane JV, Hamilton DF, MacDonald DJ, Ellis C, Howie CR. Factors that shape the patient's hospital experience and satisfaction with lower limb arthroplasty: an exploratory thematic analysis. BMJ Open. 2016; 6:e010871.
40. Wise BL, Liu F, Kritikos L, Lynch JA, Parimi N, Zhang Y, et al. The association of distal femur and proximal tibia shape with sex: The Osteoarthritis Initiative. Semin Arthritis Rheum. 2016; 46:20–26. [PubMed: 27039962]
41. Arnold AS, Komattu AV, Delp SL. Internal rotation gait: a compensatory mechanism to restore abduction capacity decreased by bone deformity. Dev Med Child Neurol. 1997; 39:40–44. [PubMed: 9003728]
42. Powers CM. The influence of altered lower-extremity kinematics on patellofemoral joint dysfunction: a theoretical perspective. J Orthop Sports Phys Ther. 2003; 33:639–646. [PubMed: 14669959]

43. Javaid MK, Lane NE, Mackey DC, Lui LY, Arden NK, Beck TJ, et al. Changes in proximal femoral mineral geometry precede the onset of radiographic hip osteoarthritis: The study of osteoporotic fractures. Arthritis Rheum. 2009; 60:2028–2036. [PubMed: 19565486]

44. Mills HJ, Horne JG, Purdie GL. The relationship between proximal femoral anatomy and osteoarthrosis of the hip. Clin Orthop Relat Res. 1993:205–208.

45. Coskun Benlidayi I, Guzel R, Basaran S, Aksungur EH, Seydaoglu G. Is coxa valga a predictor for the severity of knee osteoarthritis? A cross-sectional study. Surg Radiol Anat. 2015; 37:369–376. [PubMed: 25113012]

46. Agricola R, Leyland KM, Bierma-Zeinstra SM, Thomas GE, Emans PJ, Spector TD, et al. Validation of statistical shape modelling to predict hip osteoarthritis in females: data from two prospective cohort studies (Cohort Hip and Cohort Knee and Chingford). Rheumatology (Oxford). 2015; 54:2033–2041. [PubMed: 26139655]

47. Chang A, Hayes K, Dunlop D, Song J, Hurwitz D, Cahue S, et al. Hip abduction moment and protection against medial tibiofemoral osteoarthritis progression. Arthritis Rheum. 2005; 52:3515–3519. [PubMed: 16255022]

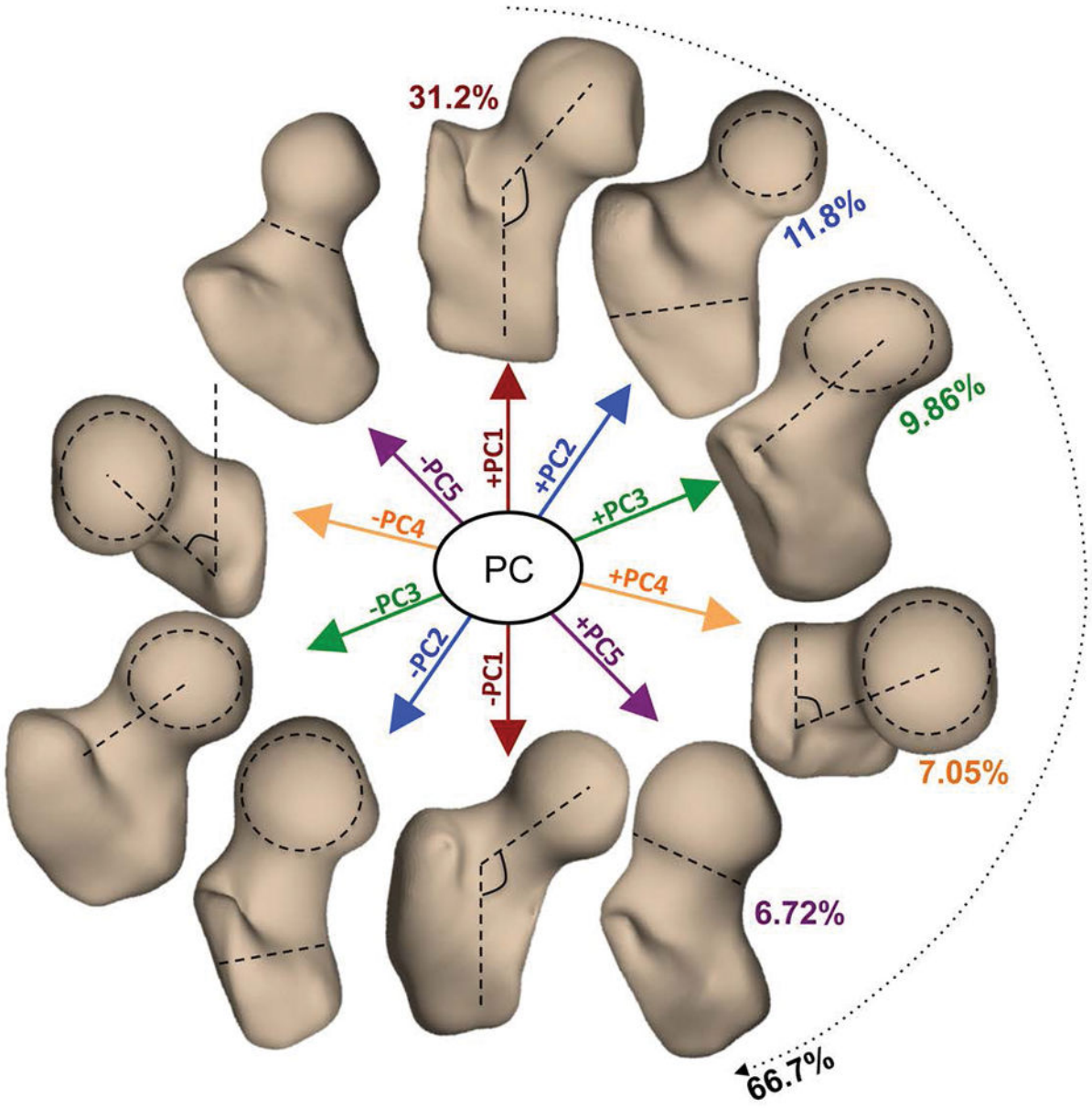

Figure 1.

Description of the first five 3D bone shape modes extracted from a dataset of 80 MRI exams. Each principal component (mode) is visualized at mean +- 3standard deviation. **PC1 (Mode 1):** neck-shaft angle in coronal plane (coxa valga/coxa vara); **PC2 (Mode 2)**: ratio between the femoral head radius and the shaft thickness; **PC3 (Mode 3):** medial–lateral length of the femoral neck; **PC4 (Mode 4):** neck shaft angle in the axial plane. **PC5 (Mode 5):** thickness of femoral neck and sphericity of the femoral head (pistol grip deformity)

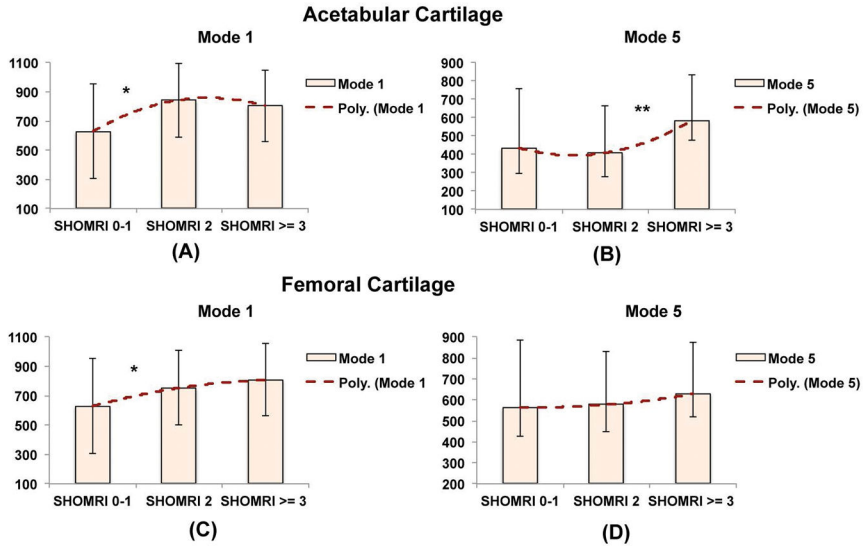

Figure 2.

Comparison of the values in mode 1 and mode 5 in subject with SHOMRI <2, SHOMRI =2, SHOMRI > 2 in acetabular (A–B) and femoral (B–C) cartilage * p-value<0.05, p value < 0.005. The y-axis in this bar graph represents the value of the shape modes 1 and 5. These are a-dimensional numbers representing the projection of each bone shape (described as a point in a multidimensional space where each dimension is one of the coordinate of each mesh's vertex) on the corresponding principal component basis.

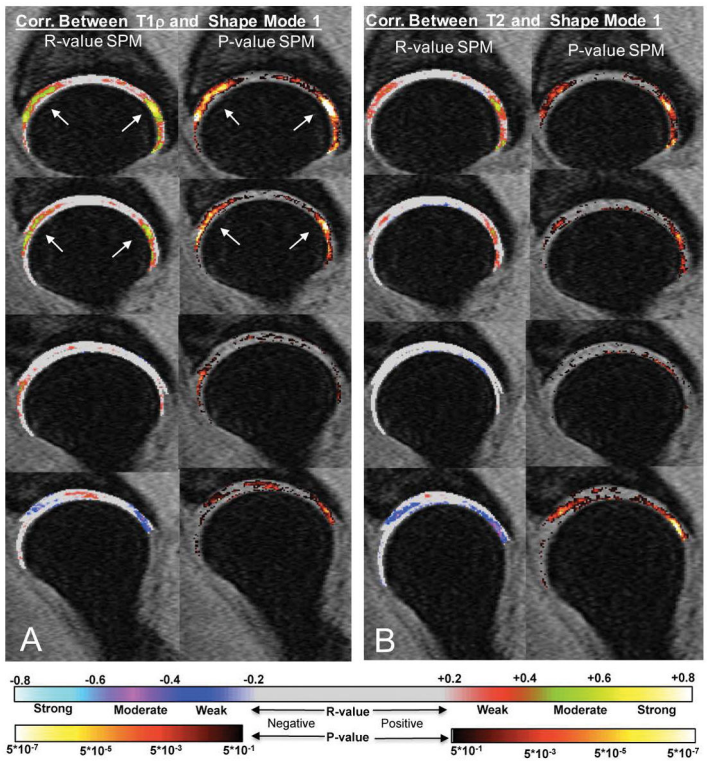

Figure 3.

R-value and P-value Statistical Parametric Maps (SPMs) representing the local correlation between bone shape feature mode 1 and the voxel based T1ρ (**A**) and T2 (**B**). Positive correlation is observed in the anterior superior and posterior superior regions demonstrating that subjects with coxa valga deformity exhibit a prolongation in relaxation times.

Table 1

Cartilage sensitive MRI hip Protocol

MRI Sequence	Sequence Parameters
3D SPGR (**MERGE**)	TR = 30.4 ms, 5 echo times (effective TE = 12.4 ms), flip angle = 15°, matrix = 512 × 512, 28 slices, slice thickness = 4 mm, field of view (FOV) = 14 cm, bandwidth (BW) = 62.5 kHz, NEX = 1, acquisition time 11:46 minutes
Combined $T_{1\rho}$ and T_2 (**MAPPS**)	FOV = 14 cm, matrix size = 256 × 128, VPS = 64, BW = 62.5 kHz, time of recovery = 1.2 sec, slice thickness = 4 mm, no gap, in-plane resolution = 0.5 mm, and acquisition time = 13:47 minutes For $T_{1\rho}$: TSL = 0/15/35/45 ms, FSL 300 Hz For T_2: TE = 0/10.4/20.8/41.7 ms

Table 2

MRI baseline characterizes evaluated with SHOMRI grading system

MR baseline Characteristics (SHOMRI)[a]			
Cartilage Lesions Total Score (N=80)			
Acetabular Cartilage		Femoral Cartilage	
Normal	47 (58.8%)	Normal	31 (38.8%)
Grade 1	9 (11.3%)	Grade 1	19 (23.8%)
Grade 2	12 (15.0%)	Grade 2	8 (10%)
Grade 3	5 (6.3%)	Grade 3	2 (2.5%)
Grade > 3	7 (8.8%)	Grade > 3	20 (25%)
Labral Total Score (N=80)		**Bone Marrow Edema Total Score (N=80)**	
Normal	6 (7.5%)	Normal	68 (85%)
Grade 1	1 (1.3%)	Grade 1	6 (7.5%)
Grade 2	3 (3.8%)	Grade 2	0 (0.0%)
Grade 3	8 (10%)	Grade 3	2 (2.5%)
Grade > 3	62 (77.5%)	Grade > 3	4 (5%)
Subchondral Cyst Total Score (N=80)			
Normal	67 (83.8%)		
Grade 1	5 (6.3%)		
Grade 2	1 (1.3%)		
Grade 3	4 (5%)		
Grade > 3	3 (3.8%)		

[a] Data expressed as Count (Percentage %).

Table 3

Summary of the results of the stepwise linear regression model of the acetabular and femoral cartilage lesion SHOMRI scores considering: (A) the first 5 mode of variation of the femoral shape as possible predictors. (B) Inclusion of the demographics and analysis of the interactions with shape (C) Ad-hoc analysis performed to compare 3D MRI-based shape feature and 2D radiograph-based geometrical measurements.

Table 3A

SHOMRI Prediction Model Obtained Without including Demographics (age, gender, BMI)

Acetabular Cartilage	**SHOMRI Score**			
	Estimate	SE	tStat	P value
Intercept	1.01006	0.16074	6..261	2.00E-08
Mode 1	0.00130	0.00050	2.460	1.60E-02
Mode 5	0.00374	0.00100	2.910	4.70E-03
Prediction Model Summary:				
Degree of Freedom: 77, RMSE: 1.66, Adjusted R^2: 0.13				
F-statistic vs constant model: 7.01, P-value: 0.0016				
Femoral Cartilage	**SHOMRI Score**			
	Estimate	SE	tStat	P value
Intercept	1.93350	0.26695	7.243	2.87E-10
Mode 1	0.00203	0.00086	2.370	2.03E-02
Mode 5	0.00477	0.00178	2.680	9.00E-03
Prediction Model Summary:				
Degree of Freedom: 77, RMSE: 2.39, Adjusted R^2: 0.12				
F-statistic vs constant model: 6.018, P-value: 0.0032				

Table 3B

SHOMRI Prediction Model Obtained including Demographics (age, gender, BMI)

Acetabular Cartilage	**SHOMRI Score**			
	Estimate	SE	tStat	P value
Intercept	−3.83200	1.28540	−2.981	3.84E-03
Age	0.04532	0.01159	3.909	1.98E-04
BMI	0.11580	0.05067	2.286	2.50E-02
Prediction Model Summary:				

Degree of Freedom: 77, RMSE: 1.38, Adjusted R^2: 0.13

F-statistic vs constant model: 11.1, P-value: 5.78E-05

Femoral Cartilage	SHOMRI Score			
	Estimate	SE	tStat	P value
Intercept	−2.07990	0.87471	−2.378	1.99E-02
Age	0.08597	0.01811	4.748	9.48E-06
Mode 1	0.00411	0.00266	−1.546	1.26E-01
Age*Mode1	0.00013	0.00006	2.286	2.51E-02

Prediction Model Summary:

Degree of Freedom: 77, RMSE: 2.15, Adjusted R^2: 0.28

F-statistic vs constant model: 11.3, P-value: 3.4E-06

Table 3C

SHOMRI Prediction Model Obtained Including MRI-based shape feature and x-Ray geometrical measurements

Acetabular Cartilage	SHOMRI Score			
	Estimate	SE	tStat	P value
Intercept	1.01670	0.16819	6.045	4.83E-08
Mode 1	0.00122	0.00054	2.256	2.69E-02

Prediction Model Summary:

Degree of Freedom: 80, RMSE: 1.5, Adjusted R^2: 0.05 F-statistic vs constant model: 5.09.1, P-value: 0.0269

Intercept	−1.33590	0.64198	−2.081	4.08E-02
Alpha Angle	0.03976	0.01090	3.649	4.81E-04
Mode 5	−0.01059	0.00449	−2.360	2.09E-02
Alpha Angle*Mode 5	0.00023	0.00008	2.960	4.11E-03

Prediction Model Summary:

Degree of Freedom: 80, RMSE: 1.35, Adjusted R^2: 0.23 F-statistic vs constant model: 9.2, P-value: 2.88E-05

Femoral Cartilage	SHOMRI Score			
	Estimate	SE	tStat	P value
Intercept	20.73900	7.17090	2.892	4.97E-03
Neck Sheft Angle	0.14368	0.05480	−2.622	1.05E-02
Mode 1	0.00175	0.00086	2.031	4.57E-02

Prediction Model Summary:

Degree of Freedom: 80, RMSE: 2.39, Adjusted R^2: 0.11 F-statistic vs constant model: 6.02, P-value: 0.00371

Intercept	−1.56780	1.10850	−1.414	1.61E-01
Alpha Angle	0.06200	0.01889	3.282	1.54E-03

Prediction Model Summary:

Degree of Freedom: 80, RMSE: 2.39, Adjusted R^2: 0.11 F-statistic vs constant model: 10.8, P-value: 0.00154

Table 4

Summary of the results of the voxel based Pearson partial correlation between the first 5 bone shape modes and the T1ρ/T2 relaxation times. The table reports: percentages of voxels showing significance (PSV), average R-values and P-value within the significant cluster

Acetabular Cartilage		**T1ρ Relaxation Times (ms)**			**T2 Relaxation Times (ms)**		
		PSV (%)	**R value**	**P value**	**PSV (%)**	**R value**	**P value**
Positive Correlations	Mode 1	29.05%	0.365	0.010	17.63%	0.318	0.013
	Mode 2	10.93%	0.272	0.022	9.96%	0.269	0.021
	Mode 3	2.17%	0.268	0.029	3.26%	0.267	0.024
	Mode 4	5.01%	0.269	0.026	6.52%	0.264	0.024
	Mode 5	1.45%	0.263	0.028	1.93%	0.279	0.019
Negative Correlations	Mode 1	6.22%	−0.298	0.0174	6.76%	−0.317	0.014
	Mode 2	1.21%	−0.267	0.0245	0.42%	−0.275	0.022
	Mode 3	1.15%	−0.262	0.0269	0.97%	−0.252	0.030
	Mode 4	2.54%	−0.288	0.0198	1.51%	−0.263	0.027
	Mode 5	3.32%	−0.262	0.0266	5.68%	−0.241	0.025
Femoral Cartilage		**T1ρ Relaxation Times**			**T2 Relaxation Times**		
		PSV (%)	R value	P value	PSV (%)	R value	P value
Positive Correlations	Mode 1	34.46%	0.386	0.008	14.97%	0.330	0.011
	Mode 2	10.84%	0.278	0.021	6.07%	0.272	0.021
	Mode 3	1.99%	0.248	0.032	2.19%	0.252	0.027
	Mode 4	2.54%	0.283	0.020	3.28%	0.253	0.026
	Mode 5	6.66%	0.262	0.026	3.88%	0.247	0.029
Negative Correlations	Mode 1	3.68%	−0.320	0.012	15.07%	−0.317	0.014
	Mode 2	1.89%	−0.277	0.021	5.07%	−0.275	0.020
	Mode 3	0.75%	−0.254	0.032	1.69%	−0.252	0.026
	Mode 4	9.10%	−0.279	0.021	5.42%	−0.263	0.023
	Mode 5	0.10%	−0.258	0.025	0.94%	−0.241	0.032

Table 5

A) Summary of the results of the stepwise linear regression model of the (i) Peak Hip internal rotation angle (ii–iii) Peak hip adduction moment and impulse (just significant models are reported),. (B) Summary of the results of the stepwise linear regression model of the results of the range of motion tests (hip internal angle and hip flection angle). Demographics, mode 1 and mode 5 were considered as possible predictors for both A and B analyses.

Table 5A

	Peak Hip Internal Angle (degree)		**Biomechanics**		
		Estimate	SE	tStat	P value
Biomechanics Prediction Model	Intercept	4.50340	0.51855	8.685	7.27E-13
	Mode 5	−0.00713	0.00339	−2.102	3.90E-02
	Prediction Model Summary:				
	Degree of Freedom: 73, RMSE: 4.49, Adjusted R^2: 0.045				
	F-statistic vs constant model: 4.42, P-value: 0.039				
	Peak Hip Adduction Moment (Nm/kg)		**Biomechanics**		
		Estimate	SE	tStat	P value
	Intercept	0.77511	0.08957	8.654	9.24E-13
	Gender	0.16223	0.05734	2.829	6.04E-03
	Mode 1	0.00019	0.00009	2.116	3.78E-02
	Prediction Model Summary:				
	Degree of Freedom: 73, RMSE: 0.24, Adjusted R^2: 0.12				
	F-statistic vs constant model: 5.69, P-value: 0.0051				
	Peak Hip Adduction Impulse(Nm*ms/kg)		**Biomechanics**		
		Estimate	SE	tStat	P value
	Intercept	244.9	30.5	8.028	1.36E-11
	Gender	46.21300	19.546	2.367	2.06E-02
	Mode 1	0.06750	0.03129	2.157	3.43E-02
	Prediction Model Summary:				
	Degree of Freedom: 73, RMSE: 84, Adjusted R^2: 0.114				
	F-statistic vs constant model: 4.65, P-value: 0.0126				

Table 5B

	Hip Internal Angle (degree)	Active Range of Motion Tests			
		Estimate	SE	tStat	P value
Active Range of Motion Prediction Model	Intercept	31.59400	1.35	23.29	2.98E-33
	Mode 5	−4.93660	1.87	−2.63	1.06E-02
	Prediction Model Summary:				
	Degree of Freedom: 65, RMSE: 7.67, Adjusted R^2: 0.0823				
	F-statsitc vs constant model: 6.92, P-value: 0.0106				